Separation and Purification Technology 398 (2026) 138125

Contents lists available at ScienceDirect

Separation and Purification Technology

journal homepage: www.elsevier.com/locate/seppur

Quaternary ammonium–modified cellulose fibers can enhance wastewater treatment performance under challenging conditions

Owen Armstrong [a], Masashi Kaneda [a,*], Georgina Kalogerakis [a], Mathieu Lapointe [b], Nathalie Tufenkji [a,c,*]

[a] Department of Chemical Engineering, McGill University, Québec H3A 2A7, Canada
[b] Department of Construction Engineering, École de technologie supérieure – University of Québec, Québec H3C 1K3, Canada
[c] United Nations University Institute for Water, Environment and Health, Richmond Hill, Ontario L4B 3P4, Canada

ARTICLE INFO

Editor name: Prof. G. Chen

Keywords:
Coagulation-flocculation
Primary treatment
Water pollution
Water management
Water quality
Sustainability

ABSTRACT

Wastewater treatment is challenged by refractory contaminants and rising water demand, while conventional coagulation-flocculation suffers from low throughput and is sensitive to the influent water conditions. Cellulose fibers can act as super-bridging agents offering enhanced turbidity removal when used in conjunction with traditional coagulants and flocculants. However, the chemical modification of cellulose fibers and their performance under challenging influent conditions remain largely unexplored. In this study, recycled cellulose fibers are modified with cationic quaternary ammonium groups, imparting a positive charge that can improve treatment performance for a wider range of water matrices including varying influent pH, ionic strength, and turbidity. Modified fibers achieve turbidity below 5 NTU across all influent pHs (7.0–8.9) and turbidities (62–285 NTU) tested, while pristine fibers show that the target turbidity of 25 NTU is not reached when the influent pH or turbidity exceed 8.2 or 130 NTU, respectively. Additionally, modified fibers achieve the target turbidity of 25 NTU even in the presence of an additional 20 mM NaCl, while pristine fibers cannot reach this target at an additional 10 mM NaCl. Furthermore, the modified fibers enhance the removal of metals such as Zn, Cr, Fe, and Pb through the incorporation of metal hydroxide precipitates within fiber-based flocs. Overall, pristine and modified fiber-enhanced treatments remove 52% and 65% of metals, respectively, compared to 39% with the conventional method. Therefore, modified cellulose fibers represent a promising strategy for enhancing coagulation-flocculation treatment performance.

1. Introduction

Water scarcity is a global crisis, affecting roughly half of the world's population at some point during the year [1]. Improperly managed wastewater exacerbates this challenge by polluting freshwater supplies and increasing pressure on limited water reserves. When discharged, untreated wastewater contributes to eutrophication, oxygen depletion, and biodiversity loss in aquatic ecosystems [2–4]. Effective wastewater treatment is therefore essential to protect both environmental and human health. However, current global estimates suggest that only 52% of wastewater is treated, largely due to a lack of collection and treatment infrastructure [5]. This issue is expected to intensify with increasing temperatures, rapid population growth, urbanization, and industrialization, all of which increase wastewater production and the risk of sending untreated discharges to the environment [6]. Therefore, technologies that reduce costs and improve water throughput during wastewater treatment are necessary for addressing the imminent global water crisis.

The coagulation-flocculation process is the most commonly used physicochemical method in wastewater treatment plants [7]. In this process, a hydrolyzing metal coagulant is used in conjunction with a polymeric flocculant to destabilize suspended particles and facilitate floc formation and subsequent settling. Common coagulants such as aluminum or ferric sulfate dissolve in water to release trivalent metal ions, which hydrolyze to form hydroxide species that neutralize suspended particle charges and facilitate the precipitation of dissolved substances [8]. Following coagulation, high-molecular weight synthetic polymers such as polyacrylamide (PAM) are added as flocculants to increase floc sizes through attachment of clumped particles on their surface [9]. Although widely used, the coagulation-flocculation process

* Corresponding author at: Department of Chemical Engineering, McGill University, Québec H3A 2A7, Canada.
E-mail addresses: masashi.kaneda@mail.mcgill.ca (M. Kaneda), nathalie.tufenkji@mcgill.ca (N. Tufenkji).

https://doi.org/10.1016/j.seppur.2026.138125
Received 24 February 2026; Received in revised form 14 April 2026; Accepted 20 April 2026
Available online 21 April 2026
1383-5866/© 2026 The Authors. Published by Elsevier B.V. This is an open access article under the CC BY-NC-ND license (http://creativecommons.org/licenses/by-nc-nd/4.0/).

is highly sensitive to influent water characteristics, including pH and ionic strength, which strongly influence floc size, strength, and structure [10,11]. Moreover, residual coagulants and flocculants that accumulate in sludge can contribute to landfill toxicity and limit the quality of sludge-based agricultural fertilizer [7]. These challenges motivate the development of novel strategies to advance conventional treatment processes.

Cellulose-based technologies such as filtration media [12], advanced membranes [13], and nanofibrous adsorbents [14,15] represent a sustainable class of water remediation solutions as they are both renewable and biodegradable. Among them, fibrous cellulose materials have recently been developed to enhance conventional coagulation-flocculation processes [7,16]. When cellulose fibers are introduced in conjunction with traditional coagulants and flocculants, the resulting flocs settle faster due to their increased size and density, and the treated water is significantly less turbid [7]. In this context, the cellulose fibers act as a flocculation aid by physically bridging and enmeshing destabilized particles and microflocs into larger, more rapidly settling aggregates, and have therefore been termed "super-bridging agents" [7,16]. This mechanism is fundamentally distinct from that of bio-flocculants (e.g., starch, chitosan), which are typically dissolved or colloidal biopolymers that adsorb onto particle surfaces and promote aggregation through polymer bridging at the molecular scale [17–20]. In contrast, super-bridging agents are discrete, macroscopic structures (typically 1–2 mm in length and 10–30 μm in diameter) that form a physical network capable of capturing particles and precipitates over much larger length scales [7,16]. This fiber-based approach has practical value in industry as the rapid settling time of the super-sized flocs produced using cellulose allows for a larger throughput and thus, an increased capacity without the addition of ballast media [7]. Additionally, the super-sized flocs can facilitate the use of screening-based floc separation, reducing the requirement for a large settling tank [7]. Compared to other technologies for the removal of suspended solids such as electrocoagulation [21], the fiber-based strategy can be implemented directly within existing settling tanks, which are used in more than 70% of wastewater treatment plants in North America [7].

While the fiber-enhanced approach to primary wastewater treatment has shown promise, important gaps in the literature remain. Despite the vast potential to functionalize cellulose with a variety of functional groups for targeting specific contaminants, few studies have assessed surface-modified cellulose fibers within the proposed context [16,22]. In one example, iron oxide grafted fibers improved phosphorus removal and enabled a reduced coagulant dosage when the fibers were reused, but showed minimal improvement of the removal of model suspended solids compared to pristine fibers [22]. In another example, fibers grafted with patches of silica demonstrated improved settling compared to the original cellulose material due to the increased density of the fibers [7]. However, the potential to enhance performance by tuning the electrostatic interaction of the fibers via covalent functionalization has yet to be explored. Moreover, the influence of key water quality parameters such as pH, ionic strength, and initial turbidity on the performance of the fiber-based strategy has not been systematically evaluated.

The objective of this work is to develop a proof-of-concept quaternary ammonium-modified fibrous material for use in wastewater treatment, and to evaluate its efficacy over a range of influent conditions. This represents the first use of a covalently functionalized cellulose fiber for use as a super-bridging agent and aims to highlight the role of the fiber surface charge in facilitating turbidity removal via the use of a well-established functionalization strategy (Table S1). First, the optimal concentration and degree of oxidation of modified fibers for turbidity removal in synthetic wastewater are determined. Then, to gain mechanistic insight into the improved performance with modified fibers, the floc size and settling rate for the (i) conventional, (ii) pristine fiber-enhanced, and (iii) modified fiber-enhanced treatment strategies are systematically compared. The robustness of this fiber-enhanced treatment is demonstrated by evaluating the turbidity of the treated water after floc settling (settled turbidity) for various influent water conditions, namely pH, ionic strengths, and turbidities, as well as in real municipal wastewater. The use of a screen to separate the fiber-based flocs from the treated water is evaluated under both typical conditions and challenging influent conditions characterized by high pH and high turbidity. Finally, the removal of metals is evaluated to further demonstrate the performance of this novel proof-of-concept fibrous material for wastewater treatment.

2. Materials and methods

2.1. Fiber preparation and modification

Recycled cardboard was used as a starting material to prepare a suspension of cellulose fibers. Cardboard was torn into 5 cm pieces and soaked in warm tap water for 5 min before blending for 7 s in a Ninja blender at 40 g/L. The resulting suspension was poured over a 160 μm stainless steel sieve and rinsed in deionized (DI) water (Type 3, Milli-Q) for 60 s before excess water was pressed out of the fibers. To prepare cellulose fibers modified with quaternary ammonium groups, a method was adapted from an existing work which produced modified nanocrystalline cellulose by oxidation with (meta)periodate followed by quaternary ammonium functionalization with (2-hydrazinyl-2-oxoethyl)-trimethylazanium chloride (i.e., Girard's reagent T) [23]. By reducing the duration of the periodate oxidation from 24 h to 2 h or less, and forgoing a hot water post-treatment step, the cellulose fibers maintain their length mostly between 1 and 2 mm. All chemicals were purchased from Sigma-Aldrich unless otherwise noted. First, 5.33 g sodium (meta)periodate ($NaIO_4$) and 15.6 g sodium chloride (NaCl, Thermo Fisher Scientific) were dissolved in 179 mL of DI water in a 500 mL flask covered in aluminum foil. Then, 91 g of a blended cardboard slurry (12 g/260 mL DI water) was added and stirred for 30, 60, or 120 min depending on the desired oxidation time (Scheme 1). This oxidation-functionalization approach was specifically selected because the oxidation time provides a direct means to control the degree of surface cationization of the fibers. As the objective of the functionalization is to modify only the fiber surface, the oxidation is kept under 120 min to avoid fibrillation [23]. The reaction was quenched with 3 mL of ethylene glycol (C_2H_6O), and the resulting oxidized fibers were poured over a 160 μm sieve and rinsed for 10 min in DI water. To induce the quaternary ammonium functionalization of cellulose, oxidized fibers underwent a Schiff base reaction (Scheme 2) with Girard's reagent T (GT, Thermo Fisher Scientific) [24]. Fibers were stirred for 24 h at a ratio of 1 g dry fibers: 4.8 g NaCl: 2 g GT: 320 g DI water with the pH of the suspension adjusted to 4.5 with 1 M HCl. The resulting modified fibers were washed over a 160 μm sieve and rinsed for 5 min using DI water.

2.2. Characterization of fibers

To determine the length of pristine and modified fibers, a diluted suspension of fibers was left to dry on a glass Petri dish at 60 °C for 24 h. Then, images of fibers were collected with a stereomicroscope (Olympus, SZX16) at 20× magnification. For each fiber type, at least 200 individual fibers were traced in ImageJ. Similarly, a diluted suspension of each fiber was left to dry on a microscope slide for IR analysis. The IR spectra of each fiber was collected on a mIRage-R (Photothermal Spectroscopy Corp.) instrument equipped with an IR pump beam (MIRcat 2400, Daylight) covering 1800–800 cm^{-1} and 3000–2650 cm^{-1} and a 532 nm probe laser. The probe power and IR power were set to 10.7% and 20%, respectively. The spectrum in the presented figures is an average of at least three measured spectra per fiber.

An electrokinetic analyzer (EKA, SurPASS 3, Anton Paar GmbH) equipped with a cylindrical cell was used to evaluate the surface charge (zeta potential) of the fibers. The streaming potential was measured at room temperature as a function of the pressure decay in the cylindrical

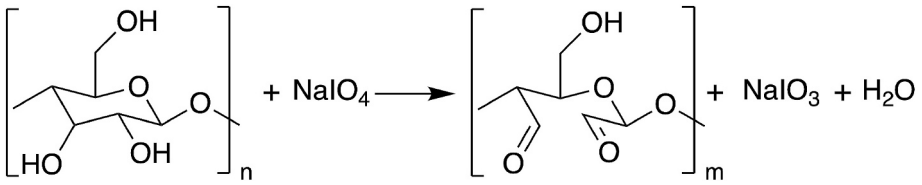

Scheme 1. Periodate oxidation of cellulose (m < n) (note that oxidation does not occur on all glucose units due to the oxidation time used in this study).

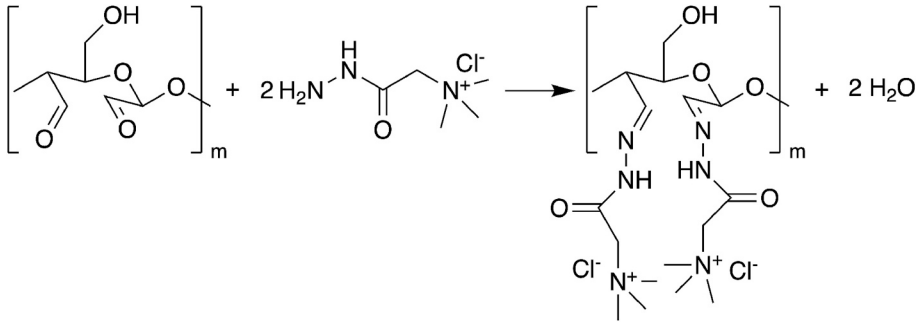

Scheme 2. Quaternary ammonium modification of oxidized cellulose (note that attaching two cationic groups to the same glucose unit is unlikely due to steric hindrance).

cell while the electrolyte solution was pumped through. The relationship between the streaming potential, measured with two Ag/AgCl electrodes, and the zeta potential was determined using the Helmholtz–Smoluchowski Eq. [25]. The electrolyte consisted of synthetic wastewater (SWW) prepared according to the recipe presented in Section 2.3, excluding the silica, urea, peptone, and meat extract. The pH of the electrolyte was adjusted to values between 7.1 and 8.6, meant to represent the pH of typical municipal wastewaters, with the addition of 1 M NaOH. For each data point, at least five measurements were taken.

Conductometric titration was used to determine the fibers' surface charge content by the same protocol as a previous work [23]. Briefly, a 150 mg/L suspension of fibers was titrated in DI water (pH = 6) with $AgNO_3$ (10 mM) in 0.1 mL increments. The temperature of the jar was allowed to reach 21 °C prior to the first titrant addition. The conductivity was recorded after at least 60 s of stirring on a conductivity probe (13–620-100, Accumet, Fisherbrand). Three titration curves were obtained for each type of fiber (Fig. S1).

The pristine and modified fibers were freeze dried and analyzed by X-ray Photoelectron Spectroscopy (XPS) with a Nexsa G2 Surface Analyzer (Thermo Scientific) equipped with an Al Kα X-ray source. Low resolution scans were conducted at pass energy 200 eV, whereas high resolution scans were conducted at 50 eV. The binding energies were referenced to the C1s neutral carbon peak at 284.8 eV.

2.3. Jar test procedure

Jar tests are conducted using the same protocol as previous work [22]. Ten-fold concentrated synthetic wastewater (SWW) was prepared according to OECD guidelines by combining 10 mg of magnesium sulfate heptahydrate ($MgSO_4{\cdot}7H_2O$), 20 mg of calcium chloride dihydrate ($CaCl_2{\cdot}2H_2O$), 35 mg of sodium chloride (NaCl), 0.15 g of urea (Alpha Chemicals), 0.14 g of dipotassium phosphate (K_2HPO_4), 0.55 g of meat extract, 0.8 g of peptone, and 500 mL of DI water [26]. The concentrated SWW was stirred for 60 min before use and was stored at 4 °C. In jar tests, 25 mL of concentrated SWW was diluted in 225 mL of tap water at room temperature (21 °C), followed by the addition of 350 µL of a silicon dioxide suspension (40 g SiO_2/L, 1–5 µm in size) to raise the initial turbidity to 62 ± 1 NTU. The zeta potential of the silica suspension was determined with a Zetasizer Ultra (Malvern) using a DTS 1070 Cell (Fig. S3a). For experiments at different pH, the SWW was adjusted with 1 M HCl or 1 M NaOH. By default, the pH of the SWW was 7.7. To increase the ionic strength or initial turbidity, additional NaCl or SiO_2 was added, respectively, to individual jars prior to starting the jar tests.

Jar tests were conducted in 500 mL glass beakers agitated with a magnetic stir bar at 200 rpm. To start coagulation, aluminum sulfate (alum) (ALS, Kemira Water Solutions Canada, Inc.) was added and mixed for 2 min. Then, anionic polyacrylamide (aPAM, molecular weight > 10^6 g/mol, anionic charge density < 5%) (Hydrex 3511, Veolia) was added in two equivalent doses one minute apart to prevent floc breakage for a total treatment time of 4 min (Fig. 1) [27]. The aPAM solution was prepared by dissolving 50 mg of aPAM in 100 mL of DI water in a fume hood and was used within one month of preparation. For treatment involving fibers, the fibers are added in a single dose, 15 s before the first addition of aPAM. The turbidity was measured using a TB 300 IR turbidimeter (Lovibond) with 10 mL of water. For the settled turbidity experiments, water was sampled 2 cm from the surface after 30 s and 180 s of settling. Select experiments were conducted with humic acid spiked synthetic wastewater, where the humic acid stock was prepared by dissolving 50 mg of humic acid (Sigma-Aldrich, # BCCB6671) in 20 mL of DI water and 300 µL of 1 M NaOH and mixing overnight to ensure complete dissolution. For the screened turbidity measurements, the sample was collected by submerging a screen basket with an aperture between 500 and 5000 µm into the water while stirring continued. The sampling pipette was cut with scissors 1 cm from the tip to ensure there was no accidental filtration of flocs during turbidity measurements. Representative images of the jars after 180 s of settling were taken using a smart phone camera. A visual representation of the jar test procedure with and without fibrous super-bridging agents is provided in Fig. 1. In order to optimize the parameters for conventional treatment, a 25 NTU setpoint was used as it is equivalent to the maximum limit of total suspended solids (TSS) for treated wastewater in Québec (Canada) (Fig. S3b, 25 mg TSS/L) [28].

2.4. Floc size and settling rate determination

Floc settling rate was determined using a similar approach as previous work [29]. After 180 s of settling, the jar was stirred gently to resuspend settled flocs which were then individually transferred with a plastic pipette to the top of a 500 mL graduated cylinder filled with tap water. A stopwatch was used to determine the time required for 30 flocs

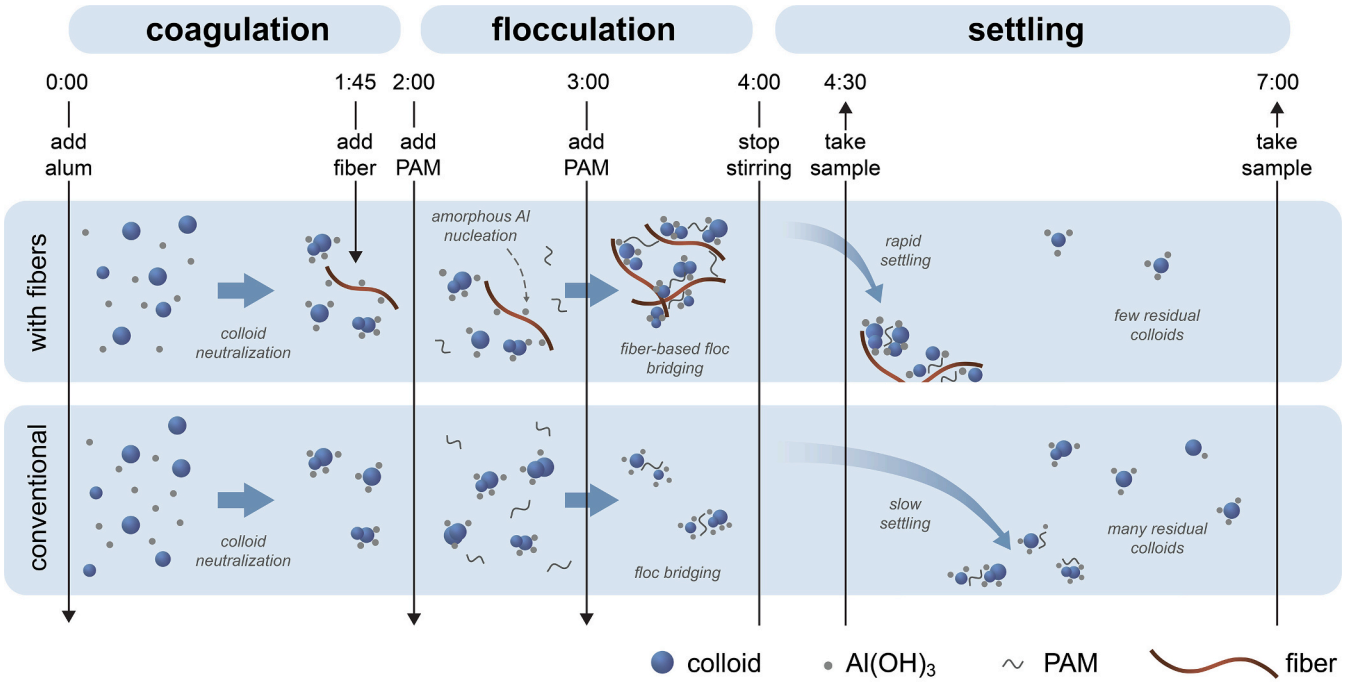

Fig. 1. Overview of jar test procedure and underlying chemistry during coagulation, flocculation, and settling for conventional and fiber-enhanced treatment strategies. Values above the diagram represent the timing (min:s) for the three-step jar test procedure used in all experiments.

to reach the bottom of the cylinder which corresponded to a distance travelled of 24.5 cm. To determine the area of flocs, separate jar tests were conducted and again the jar was gently stirred after 180 s settling and 30 individual flocs were transferred to a Petri dish. After leaving to air dry, the flocs were imaged using a stereo microscope (Olympus, SZX16) at 20× magnification. The circumference of the flocs was traced in ImageJ to compute a representative area. To determine differences in the floc size and settling rate, statistical analyses were conducted in MATLAB using the Statistics and Machine Learning Toolbox. As data were not normally distributed (Anderson Darling test), the non-parametric Kruskal-Wallis test was used, followed by the MATLAB multcompare function to identify significant differences.

2.5. Jar tests in real wastewater influent

The use of conventional, pristine fiber-enhanced, and modified fiber-enhanced treatments were evaluated in real municipal wastewater collected at the influent of the Sainte-Catherine wastewater treatment plant (Sainte-Catherine, Québec, Canada, water properties in Table S2). For tests in real wastewater, a TL2350 turbidimeter (HACH) was used to measure the turbidity after 30 s and 180 s of settling. Total suspended solids (TSS) was determined by the US EPA Gravimetric method (Section 2540D) [30] with glass microfibre filters (pore size 0.7 μm, GE Healthcare Life Sciences, Whatman).

2.6. Quantifying removal of metals

All metals were purchased from AnalytiChem with stock concentration 1000 mg/L in 2% nitric acid (HNO_3). For jar tests meant to elucidate the removal of metals, metal stocks were added to each jar to reach a concentration of 0.5 mg/L of Ni, Fe, and Zn, and 0.05 mg/L of Cr, Pb, and Mn. These concentrations are of similar magnitude and relative abundance than those observed in real wastewater influents [31]. Each jar was adjusted to pH 7.7 using 1 M NaOH before initiating the coagulation-flocculation processes. A 10 mL sample was collected in a polypropylene tube (DigiTUBE) after 30 s and 180 s of settling for metal analysis. Samples were acidified using nitric acid (ThermoFisher Scientific, 67%) and subsequently digested at 95 °C for 1 h in a DigiPREP (SCP Science). Then, samples were subject to vacuum filtration through hydrophilic Teflon filters (pore size 0.45 μm, Fisherbrand) before injection in an iCAP 6000 series ICP Spectrometer (ThermoFisher Scientific) to determine the concentration of each metal in the sample. To confirm the success of the acidification and digestion procedure, as well as to ascertain whether there were significant experimental losses of metals during the experiment, a control test was conducted (Fig. S4). Following jar tests for the removal of metals with modified fibers, the sludge was collected, freeze dried, and then analyzed by XPS by the method described in Section 2.2.

3. Results and discussion

3.1. Characterization of pristine and modified cellulose

The synthesis of modified cellulose was conducted by periodate oxidation followed by quaternary ammonium functionalization with Girard's reagent T. The length distribution, zeta potential, surface charge content, and IR spectra of pristine fibers and modified fibers obtained via the three different oxidation times are shown in Fig. 2. The average length of both pristine and modified fibers is ~1600 μm, as shown in Fig. 2a, suggesting that the periodate oxidation step does not significantly alter the physical integrity of fibers despite cleavage of some adjacent hydroxyl groups on the cellulose chain [23].

The zeta potential of pristine (unmodified) cellulose was between −6 and − 7 mV for the range of pH studied. The zeta potential for modified cellulose oxidized for 60 and 120 min is consistently greater than the unmodified starting material, confirming the partial cationization of the modified fiber surface. At pH 7, the zeta potential of the modified fibers increased from −2.7, to −0.1, to 1.9 mV, with increasing oxidation time (30, 60, 120 min). The zeta potential of all functionalized fibers decreased slightly with increasing pH.

The average charge content on the fibers' surface is measured by conductometric titration to determine the concentration of quaternary ammonium groups present (Fig. 2c and Fig. S1). Consistent with the results for the zeta potential, an increase in the oxidation time leads to

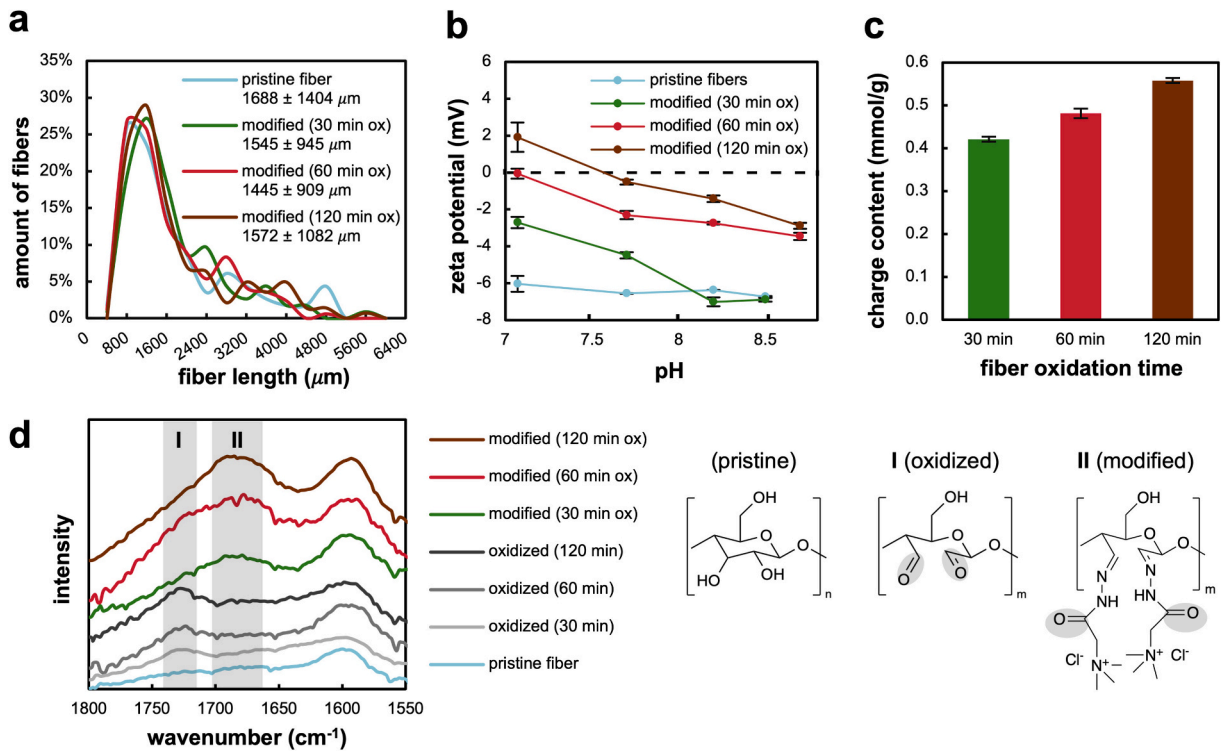

Fig. 2. Characterization of pristine, oxidized, and modified cellulose fibers oxidized for 30, 60, and 120 min. (a) Length distribution for pristine and modified fibers. (b) Zeta potential for pristine and modified fibers for varying pH, evaluated in a matrix of salts which make up SWW (28 mg/L K_2HPO_4, 7 mg/L NaCl, 4 mg/L $CaCl_2{\cdot}2H_2O$, 2 mg/L $MgSO_4{\cdot}7H_2O$). (c) Charge content of quaternary ammonium group of modified fibers, evaluated via conductometric titration with 10 mM $AgNO_3$. (d) IR spectra for pristine, oxidized, and modified fibers. Signals associated with oxidized and modified fibers are indicated by the grey panels labelled I and II, respectively.

an increasing charge content, from 0.42 mmol/g for 30 min oxidized to 0.48 and 0.56 mmol/g for 60 min and 120 min oxidized, respectively. This demonstrates that by altering the oxidation time it is possible to tune the degree of cationization on the fibers' surface. These values are consistent with previous work which synthesized cationic nanocrystalline cellulose and reported a charge content of 1.68 mmol/g after a much longer (24 h) oxidation time [23].

The IR spectra for the pristine fibers, oxidized intermediate fibers, and modified fibers are shown in Fig. 2d. The oxidized cellulose displays a new peak at 1725 cm^{-1} (peak I) demonstrating the presence of the C═O aldehyde group [32]. The modified cellulose no longer has a peak at 1725 cm^{-1} and instead has a broad peak at 1680 cm^{-1} (peak II) associated with the carbonyl group from Girard's reagent T [23], confirming that the reaction was successful in preparing modified cellulose with significant conversion of aldehyde groups. Additionally, XPS of pristine and modified fibers (60 min oxidized) confirms the presence of nitrogen on the fibers' surface due to the reaction (Schemes 1, 2) (Fig. S2).

3.2. Optimization of jar test parameters

Prior to evaluating the robustness of the wastewater treatment strategies, the mixing speed as well as the coagulant and flocculant concentration were optimized based on the conventional treatment strategy with 180 s of settling. The ideal mixing speed was determined to be 200 rpm (Fig. S5), and the optimal alum and aPAM dosages were adjusted until the conventional treatment method yielded 25 NTU after 180 s settling and were 48 mg/L and 0.5 mg/L, respectively (Fig. S6). These three parameters (stir speed = 200 rpm, coagulant dose = 48 mg/L, flocculant dose = 0.5 mg/L) were maintained throughout all subsequent jar tests unless otherwise indicated.

To determine the ideal synthesis conditions for the modified fibers and the ideal fiber concentration, the settled turbidity for fibers with different oxidation times and fiber concentrations was evaluated as presented in Fig. 3. The addition of modified cellulose leads to improved turbidity removal compared to pristine cellulose (unmodified) under almost all conditions tested, confirming that the surface charge of the fibers is a critical factor for fiber efficiency. Interestingly, the optimal fiber concentration for modified fibers increases with decreasing oxidation time, whereas the pristine fibers show similar turbidity removal for all concentrations between 50 and 200 mg/L. At 180 s settling, the ideal fiber concentration increases from 50 to 150 to 200 mg/L for fibers oxidized for 120 min, 60 min, and 30 min, respectively (Fig. 3b). This observation is pronounced at 30 s settling, where the fibers oxidized for 120 min show a steep increase in settled turbidity at all concentrations above 50 mg/L and perform worse than the pristine fibers at 200 mg/L (Fig. 3a). This decrease in performance at a high concentration of the modified fibers is likely the result of two competing electrostatic interactions: (i) between modified cellulose and anionic suspended particles which improves turbidity removal, and (ii) between individual charged fibers which hinders floc formation and particle settling, thus inhibiting turbidity removal. Consistent with this explanation, the lowest charge density fibers (30 min oxidation, 0.42 mmol/g) achieved optimal performance at the highest tested dosage (200 mg/L), while more highly charged fibers reached optimal performance at lower concentrations (Fig. 3). With increasing oxidation time, the higher charge content on the fibers' surface likely causes the dominant interaction to switch from turbidity removal (attraction between fibers and particles) to floc formation inhibition (repulsion between fibers). As such, increased surface charge promotes initial particle attachment but may hinder floc growth at higher fiber concentrations by limiting interfiber bridging. Due to the higher concentration of quaternary ammonium groups on the 120 min oxidized fibers (Fig. 2c and Fig. S1), it is also likely that a higher flocculant dose is required to successfully

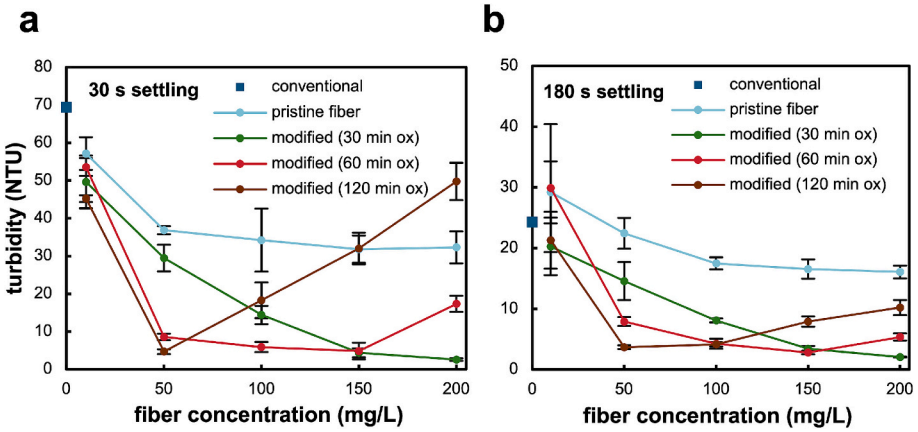

Fig. 3. Turbidity after 30 s (a) and 180 s (b) settling for varying fiber concentrations. Jar test conditions: 48 mg/L alum, 0.5 mg/L aPAM, pH = 7.7 ± 0.1, initial turbidity = 62 ± 1 NTU. The settled turbidity with conventional treatment (without fibers) is shown with a blue square symbol for comparison. Data points and error bars are calculated from the average and standard deviation of three replicates. (For interpretation of the references to colour in this figure legend, the reader is referred to the web version of this article.)

aggregate modified fibers at fiber concentrations >50 mg/L.

As the modified fibers oxidized for 60 min showed excellent turbidity removal at 30 s settling over a broad range of fiber concentrations (50–150 mg/L), the 60 min oxidation time was chosen for the subsequent experiments. These fibers performed best at concentration 150 mg/L, where the turbidity dropped to 3 NTU after 180 s settling, compared to the 17 NTU achieved with pristine fibers at the same concentration (Fig. 3b).

3.3. Understanding the mechanisms of turbidity removal via modified fibers

The residual turbidity, floc size, and floc settling behavior were compared for the conventional (no fibers) and fiber-enhanced (150 mg/L pristine and 150 mg/L modified) treatment strategies. Fig. 4a shows that the improved clarity of the treated water is visually distinct for each of the conditions tested, and that the fiber-containing sludge has a higher volume and appears less dense than the conventional sludge. The analyzed flocs with conventional treatment were all of similar size (0.82 ± 0.64 mm^2) and within an order of magnitude of typical floc sizes reported by other studies [33,34], whereas the fiber-based flocs are substantially larger, and take on a range of sizes based on the number of fibers which have become incorporated (Fig. 4b and c). As resuspending settled flocs and measuring them with 2D imaging cannot fully represent their 3-D structure, these floc sizes should be used only for relative comparison between treatments. Comparing the pristine and modified fiber-based flocs, the modified fibers had a significantly larger cross-sectional area (30.2 mm^2 compared to 12.3 mm^2 for pristine fibers) and settling rate (0.68 cm/s compared to 0.48 cm/s for pristine fibers), showing potential to match floc settling rates achieved via magnetite-ballasted flocculation [35]. As such, the short settling times (30 s and 180 s) used in this study are significantly lower than those used elsewhere, which can range from 20 min–2 h for similar coagulation-flocculation processes [36–38].

The floc images in Fig. 4b suggest a mechanistic difference in the removal of turbidity between the conventional and fiber-enhanced treatment strategy. With both types of fibers, the silica aggregates along the surface of the fibers are much smaller than those obtained via the conventional method, suggesting that instead of simply bridging silica aggregates together, the fibers accumulate small coagula on their surface. Then, after bridging induced by the flocculant, the fibers rapidly settle these attached coagula and facilitate their removal. To better understand how the surface modification of fibers leads to improved performance, jar tests were conducted excluding either SiO_2 and coagulant, coagulant and flocculant, or just flocculant, which allows for isolating the various interactions at play with both fiber types (Fig. 5).

In jar tests without any SiO_2 or coagulant (Fig. 5a), the interaction between the fibers and anionic flocculant could be isolated, as residual turbidity was solely the result of unsettled fibers in suspension. The modified fibers settled more quickly, reaching 12 NTU after 30 s compared to 30 NTU with pristine fibers, indicating that the improved performance of modified fibers could be partially attributed to an enhanced fiber-flocculant interaction (Fig. 5a). In turbid wastewater without coagulant and flocculant (Fig. 5b) it can be determined if suspended particles adhere to fibers' surface. Under these conditions, modified fibers facilitated a slight reduction in turbidity (~6%, $p < 0.05$) after 180 s of settling demonstrating the attachment of some negatively charged particles (Fig. S3a) directly to the modified fiber surface (Fig. 5b). The pristine fibers were unable to reduce turbidity under the same conditions, suggesting the direct fiber-particle interaction is unique to the fibers with quaternary ammonium functional groups (Fig. 5b). In turbid wastewater without flocculant (Fig. 5c), the interaction between coagula and fibers is isolated. After 180 s, the modified fibers achieved 36 NTU whereas pristine fibers resulted in no removal (Fig. 5c). This indicates that the modified fibers also have an improved interaction with coagulated particles. In summary, these results demonstrate that the improved performance associated with the modified fibers is due to a higher affinity for flocculant, individual particles, and destabilized coagula simultaneously, which enables the rapid formation of super-sized flocs.

3.4. Turbidity removal under challenging influent conditions

To evaluate the robustness of the fiber-enhanced wastewater treatment strategy and account for the water quality variation observed in full-scale wastewater treatment plants, jar tests were conducted over a range of influent conditions. In particular, the pH, ionic strength, and initial turbidity of the synthetic wastewater were systematically varied based on the observed properties of real wastewater, and an additional test was conducted in real wastewater. The pH from urban wastewater is typically between 7 and 8 but can also reach pH as high as 8.9 when mixed with industrial wastewater [39]. The ionic strength of wastewater influent/effluent typically ranges from 0.003 to ~0.040 M while the turbidity can exceed 250 NTU even for domestic streams [40]. A comparison between the settled turbidity after conventional, pristine fiber-enhanced, and modified fiber-enhanced treatment for the different tested conditions is presented in Fig. 6. The ideal dosage of modified fibers (150 mg/L, Fig. 3), as well as a lower dosage (50 mg/L) were used

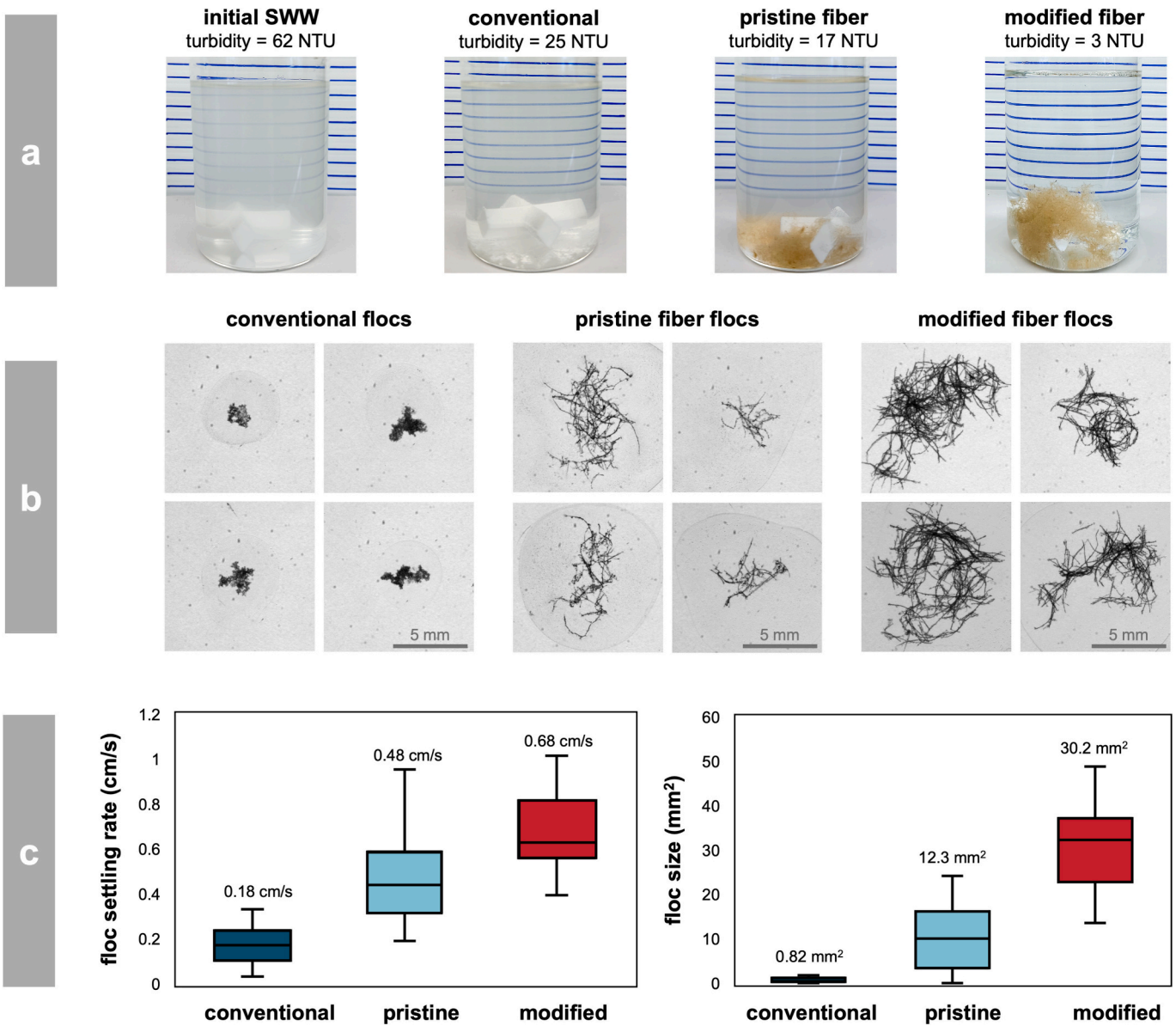

Fig. 4. Comparison of settled turbidity, floc size, and floc settling rate for conventional, pristine fiber-enhanced (150 mg/L) and modified fiber-enhanced (150 mg/L) treatment strategies. (a) Images of jars taken before treatment (leftmost) and after treatment and 180 s of settling. The turbidity values shown are obtained by sampling 10 mL of water 2 cm from the top of the jar. (b) Representative images of flocs formed via the three treatment strategies. (c) Box and whisker plots for floc settling rate (left) and floc size (right) for flocs formed via the three treatment strategies ($n = 30$). The quartiles are calculated using an inclusive median. Each condition yields a statistically different floc settling rate ($p < 0.05$) and floc size ($p < 0.01$). Jar test conditions: 48 mg/L alum, 0.5 mg/L aPAM, pH = 7.7 ± 0.1, initial turbidity = 62 ± 1 NTU.

to prevent masking the sensitivity of the fiber-based strategy to variations in the influent conditions, as well as to determine if fiber modification reduced the fiber dosage that is required for sufficient wastewater treatment.

The conventional treatment strategy shows a drastic decrease in effectiveness at pH values above 7.7, where there is no turbidity removal after 180 s settling as shown in Fig. 6a. This is expected, as the point of zero charge of precipitated aluminum hydroxide particles is near pH 8, so achieving charge neutralization and sweep flocculation of the negatively charged SiO_2 particles at pH greater than 8 is unfavorable [41]. All fiber-enhanced treatments are less impacted by increasing pH than the conventional method (Fig. 1). With 150 mg/L of modified fibers, the turbidity is well below the target value of 25 NTU at both 30 s and 180 s settling for all pHs. The ability of modified fibers to improve turbidity removal under higher pH conditions is most evident at 180 s settling, where the turbidity is less than 4 NTU at pH 8.9 when using 150 mg/L of fibers (Fig. 6a). In contrast, the pristine fiber treatment achieved a turbidity of 34 NTU, and the conventional strategy failed to remove any turbidity at this high pH condition. This suggests modified fibers may facilitate bridging between particles and any remaining aluminum hydroxide precipitates which have negative surface charge at pH 8.9 [41].

Increasing the ionic strength of the SWW with an additional 0.78 mM of NaCl (a ~6.5-fold increase in the NaCl concentration) challenged the conventional treatment method, which reached 40 NTU after 180 s settling (Fig. 6b). At higher ionic strength, the presence of ions may lead to an increase in the floc dissociation coefficient and conformational changes in the flocculant polymer both of which inhibit turbidity removal [42,43]. A similar observation has been made for the removal of TiO_2 nanoparticles during coagulation where increasing the ionic strength above 0.03 M (NaCl) reduced the performance [44]. The fiber-

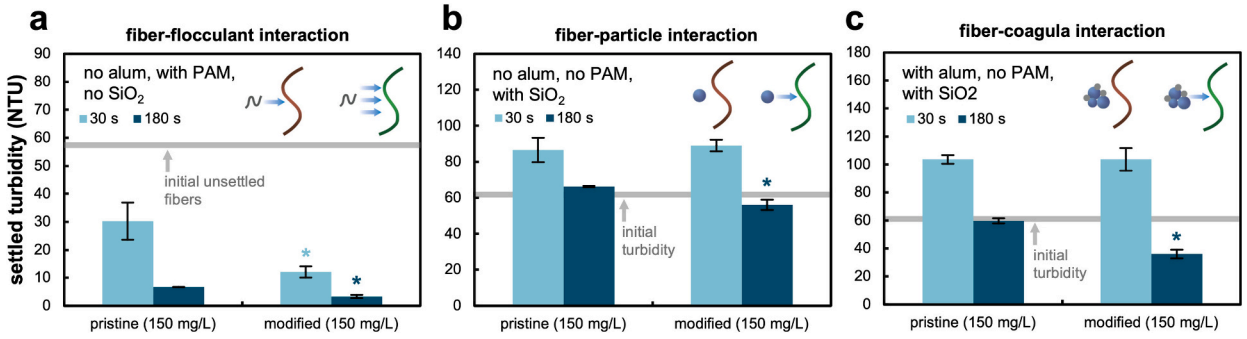

Fig. 5. Jar tests to elucidate mechanisms of modified fiber-based treatment. (a) Flocculation of pristine (150 mg/L, brown) and modified (150 mg/L, green) fibers with aPAM (0.5 mg/L). Jar tests were conducted in synthetic wastewater without SiO_2 or alum to determine the relative affinity of each fiber for the anionic flocculant. As there is no SiO_2 added, turbidity is representative of fibers in suspension (initial turbidity ~58 NTU). (b) Jar test conducted with only fibers and SiO_2, no coagulant or flocculant. (c) Jar test conducted with alum (48 mg/L) and SiO_2 but without any flocculant. Jar test conditions: pH = 7.7 ± 0.1, initial turbidity = 62 ± 1 NTU. Data points and error bars are calculated from the average and standard deviation of 3 replicates. Statistical differences ($p < 0.05$, two-tailed heteroscedastic *t*-test) between the pristine and modified fibers are shown with an asterisk above the modified fiber result. Schematic drawings show the improved interactions between the flocculant, particles, and coagula with modified fibers (green, right) compared to pristine fibers (brown, left). (For interpretation of the references to colour in this figure legend, the reader is referred to the web version of this article.)

enhanced treatment strategies were all inhibited by the increased ionic strength (Fig. 6b). At 180 s settling, the pristine fibers exceeded the target, reaching 28 NTU after an additional 9.3 mM NaCl. The modified fibers (150 mg/L) performed more robustly, only exceeding the target after 39 mM additional NaCl. This indicates that salts may interfere with the interaction between fibers and suspended solids, inhibiting their ability to promote coagulation kinetics and/or floc bridging [45]. For the modified fibers, it is likely that the inhibitory effect is the result of Cl^- screening the positively charged quaternary ammonium groups through compression of the electrical double layer, reducing their effective surface charge and weakening electrostatic interactions with negatively charged particles, however the modified fibers still outperform pristine fibers for all ionic strengths tested [46].

The residual turbidity increased linearly with initial turbidity for all treatment strategies as shown in Fig. 6c. At all initial turbidities above 62 NTU, the conventional method and pristine fiber-enhanced strategy failed to meet the settled turbidity target at 180 s settling. However, the modified fibers demonstrated good turbidity removal even when the initial turbidity was 285 NTU, achieving settled turbidity <5 NTU even at 30 s settling (i.e., 98% removal in turbidity). By contrast, the conventional method removed only 6% and 52% of turbidity at 30 s and 180 s settling at this initial turbidity, respectively. Comparatively, with advanced electrocoagulation techniques, the current and operating time must be adjusted to achieve sufficient removal for highly turbid waters [47]. This demonstrates the unique ability of the modified fibers to produce effluent water that satisfies regulatory limits subject to changes in the influent turbidity without adjusting any chemical dosages or operating parameters, which is particularly relevant during high rainfall events where increases in water flowrate and turbidity are triggered concurrently [48].

Previous work has shown that the addition of fibers enables the use of a novel screening method to facilitate floc separation due to the substantially increased floc size [7]. This method has the potential to improve treatment capacity, and reduce operational costs and capital expenditures as screening the flocs from the treated water reduces the need for a large settling tank [49]. This screening method is especially effective with modified fibers, as shown in Fig. 7. Under the standard condition (Fig. 7a) (pH 7.7, initial turbidity = 62 ± 1 NTU, no additional NaCl), the addition of modified fibers (150 mg/L) achieves the turbidity target for a screen aperture size up to 2000 μm, whereas pristine fibers, although substantially more effective than conventional treatment, required a screen mesh 4 times smaller to reach the target (500 μm). This is consistent with the representative flocs shown in Fig. 4b, where the modified fibers produced flocs with diameter ~5000 μm, whereas the smallest representative pristine fiber floc had diameter ~2500 μm, which would not be screened by a 2000 μm aperture due to deformations of the floc upon impact with the screen. This confirms that the increased floc size of modified fibers (Fig. 4) leads to a distinct improvement when separating the super-sized flocs from the treated wastewater. The improved performance of modified fibers via screening extends to high pH and high turbidity water conditions (Fig. 7b and c). At pH 8.9 and for screen sizes between 500 and 2000 μm, modified fibers consistently achieve the target whereas pristine fibers fail to achieve the target for any screen aperture size (Fig. 7b). For high turbidity water (285 NTU, Fig. 7c) the screened method is unable to achieve the turbidity target even with the smallest screen aperture (500 μm), regardless of the fiber type, likely due to an excess of silica particles in suspension. However, the improvement of the modified fibers even in highly turbid waters is still evident, highlighting the potential of these fibers to promote screening-based separation, although screen apertures less than 500 μm would be needed in these cases.

To demonstrate a more realistic application of the modified fibers, jar tests were conducted in wastewater collected from the Sainte-Catherine wastewater treatment plant (Québec, Canada) (Fig. 8). The coagulant dose for this wastewater matrix was optimized to achieve turbidity <25 NTU after 180 s of settling without fibers (Fig. S7) (2.5 mg/L alum). The best performance was achieved with modified fibers (150 mg/L) where the settled turbidity reached 18.7 and 10.3 NTU after 30 and 180 s of settling, respectively, compared to 38.5 and 23.8 NTU with the conventional method, although the pristine fibers at the same concentration achieved similar performance. This is likely due to the conductivity of this real wastewater which is 3 times higher than the synthetic wastewater (Table S2). As described previously (Fig. 6b), background salts can diminish the performance of the fiber-based treatments. For comparison, the conductivity of the real wastewater was similar to the conductivity of the synthetic wastewater with an additional 10 mM of NaCl, at which point both pristine and modified fibers were significantly inhibited (Fig. 6b and Fig. S8). In addition to ionic strength effects, the presence of additional dissolved organic matter in real wastewater may further contribute to performance limitations. Supplementary experiments with humic acid (Fig. S9) showed a similar decline in turbidity removal efficiency with increasing dissolved organic matter, suggesting that negatively charged humic substances adsorb onto the positively charged fiber surfaces, thereby reducing their effective surface charge.

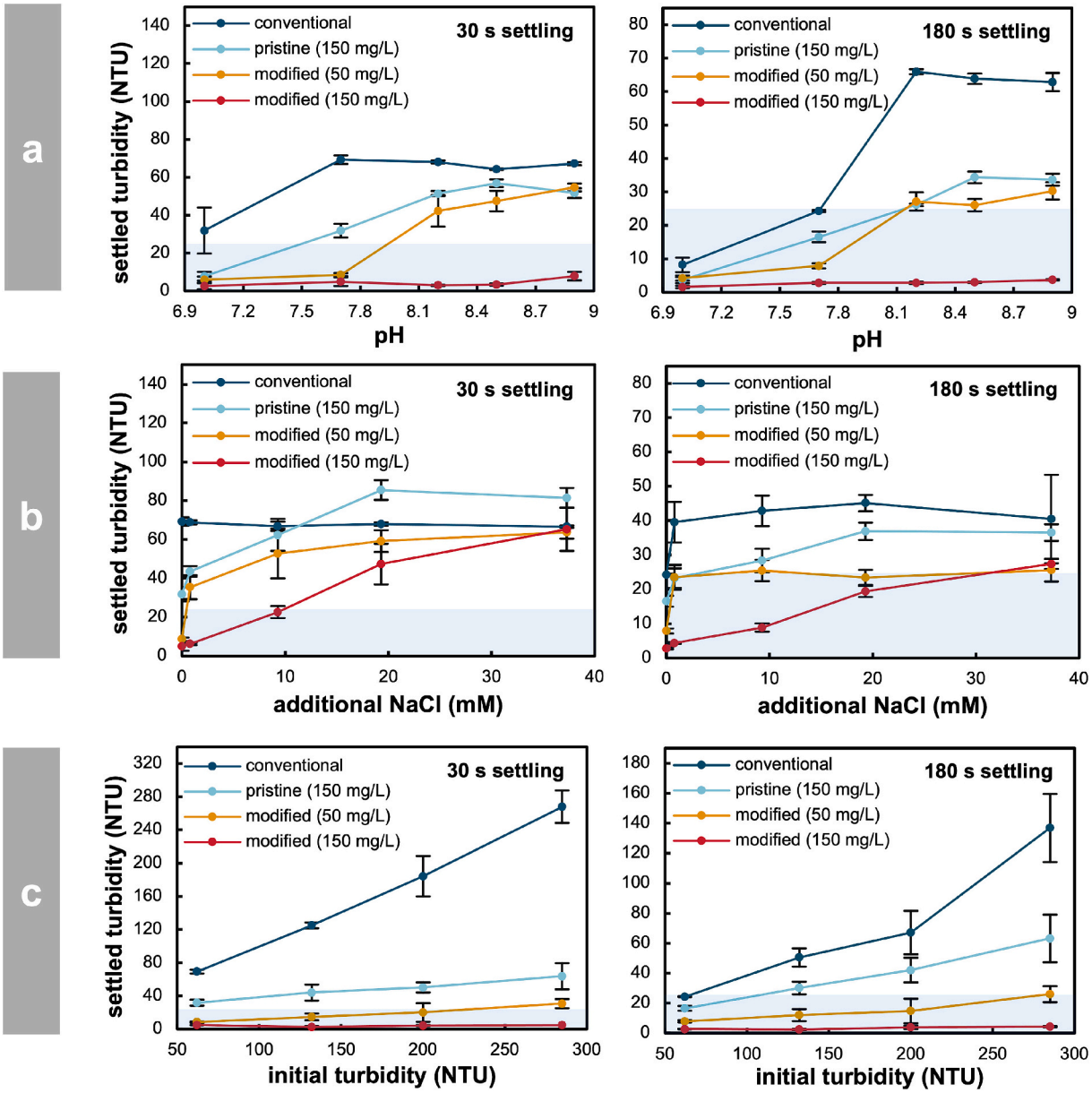

Fig. 6. Turbidity after 30 s and 180 s settling with conventional, pristine fiber-enhanced (150 mg/L), and modified fiber-enhanced (50 and 150 mg/L) treatment strategies for varying influent conditions. (a) Settled turbidity for pH between 7.0 and 8.9. (b) Settled turbidity for additional NaCl between 0 and 37 mM. (c) Settled turbidity for initial turbidity between 62 and 285 NTU. Coagulant and flocculant concentrations: 48 mg/L alum and 0.5 mg/L aPAM. Default jar test conditions unless otherwise mentioned: pH = 7.7 ± 0.1, initial turbidity = 62 ± 1 NTU. Data points and error bars are calculated from the average and standard deviation of 3 replicates. Settled turbidity target is shown in light blue. (For interpretation of the references to colour in this figure legend, the reader is referred to the web version of this article.)

3.5. Removal of metals

Metals such as Cr, Pb, and Ni are ubiquitous in wastewater effluents and are known for their carcinogenic and teratogenic effects [50]. Fig. 9a shows the removal of 39% of total spiked metals (Ni, Mn, Zn, Cr, Fe, and Pb) by the conventional method after 180 s of settling (data after 30 s settling in Fig. S10). The addition of both pristine and modified fibers improved the removal of metals compared to the conventional method. After 180 s of settling, pristine fibers improved the removal of total metals to 52%, while modified fibers (150 mg/L) improved the removal to 65%. This is likely attributed to the improved removal of metal-containing suspended solids with the fiber-based technology, as evidenced by the linear relationship between turbidity removal and total metal removal with different treatment strategies (Fig. 9b).

Metal speciation in the simulated wastewater is governed by a complex set of equilibria, wherein dissolved metals may partition among free ions, hydrolyzed species (including aqueous hydroxo-complexes and metal hydroxide precipitates), and complexes with co-existing ligands such as phosphate and sulfate [51]. While phosphate can form stronger inner-sphere complexes [52], the presence of free PO_4^{3-} ions requires higher pH [53], and sulfate is present only at low concentration ($MgSO_4{\cdot}7H_2O$ at 2 mg/L). At the current experimental pH of 7.7, metal-hydroxide formation is therefore expected to predominate over these competing interactions. Evidently, Zn, Cr, Fe, and Pb show the highest removal by all treatment strategies, whereas the removal of Ni and Mn is significantly lower (Fig. 9a). These differences can be understood in terms of the solubility of each metal hydroxide, where Zn, Cr, Fe, and Pb hydroxides are insoluble at pH 7.7 while Ni and Mn hydroxides would

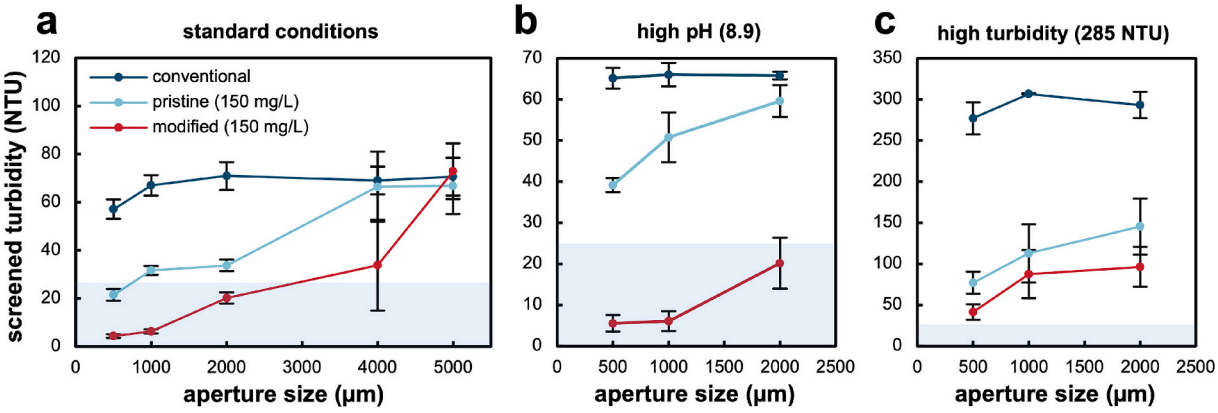

Fig. 7. Screened turbidity with conventional, pristine fiber-enhanced (150 mg/L), and modified fiber-enhanced (150 mg/L) treatment strategies. (a) Screened turbidity for various aperture sizes (500–5000 μm) under the standard wastewater condition (pH 7.7, initial turbidity = 62 ± 1 NTU, no additional NaCl). (b) Screened turbidity for various aperture sizes (500–2000 μm) in high pH wastewater (initial turbidity = 62 ± 1 NTU, no additional NaCl). (c) Screened turbidity for various aperture sizes (500–2000 μm) in high turbidity wastewater (pH 7.7, no additional NaCl). Coagulant and flocculant concentrations: 48 mg/L alum and 0.5 mg/L aPAM. Data points and error bars are calculated from the average and standard deviation of 3 replicates. Turbidity target is shown in light blue. (For interpretation of the references to colour in this figure legend, the reader is referred to the web version of this article.)

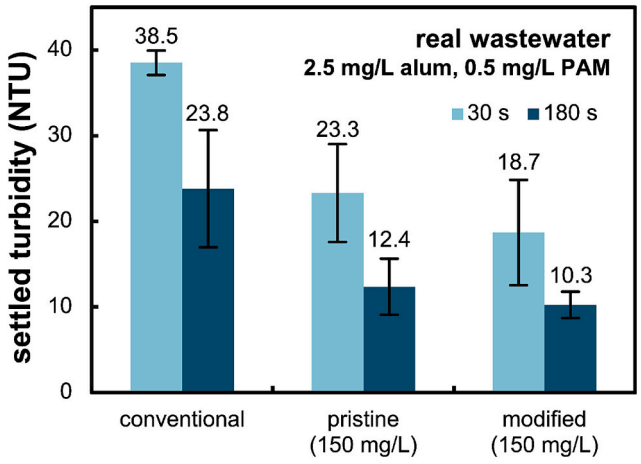

Fig. 8. Turbidity after 30 s and 180 s settling with conventional, pristine fiber-enhanced (150 mg/L), and modified fiber-enhanced (150 mg/L) treatment strategies in real wastewater. Coagulant and flocculant concentrations: 2.5 mg/L alum and 0.5 mg/L aPAM. Water conditions: pH = 6.9 ± 0.1, initial turbidity = 40.6 NTU. Data points and error bars are calculated from the average and standard deviation of 3 replicates.

remain dissolved until higher pH based on chemical equilibrium simulations in a 10 mM electrolyte [51]. For this reason, increasing linear relationships between the metal removal (%) and turbidity removal (%) are observed for Zn, Cr, Fe, and Pb, but not for Mn and Ni (Fig. S11). These strong relationships between the properties of the metal hydroxide species and the removal of each metal suggest that metal removal is primarily governed by pH-driven formation of metal hydroxide species, with the modified fibers acting to enhance the physical removal of these precipitates rather than serving as the primary adsorption sites for dissolved metals. In this context, the fibers function as a bridging and enmeshment medium that accelerate aggregation and settling.

XPS analysis was conducted on the sludge produced by treatment with 150 mg/L of modified fibers, with low- and high-resolution spectra of each metal presented in Fig. 9c-f and Fig. S12. For the metals which are removed well by the treatment (Zn, Cr, Fe, and Pb; removal ~85%), the XPS scans clearly indicate their prevalence within the fibrous sludge (Fig. 9c-f). The Zn 2p spectra (Fig. 9c) has primary peaks at 1023.2 and 1046.3 eV relating to Zn $2p_{3/2}$ and Zn $2p_{1/2}$, respectively, where the position of the Zn $2p_{3/2}$ peak indicates $Zn(OH)_2$ is the dominant species [54]. For Cr 2p (Fig. 9d), the broad Cr $2p_{3/2}$ (579.6 eV) and Cr $2p_{1/2}$ (589.0 eV) peaks suggest a combination of chromium oxide and chromium hydroxide species [55], as well as potential oxidation of Cr (III) to Cr (VI) during treatment [56,57]. However, these Cr 2p peaks also contain contributions from chromium present in the unused modified fibers (Fig. S13) which is associated to impurities in the cardboard starting material (Fig. S14). As such, the incorporation of chromium-containing species within the flocs could not be conclusively determined based on the current XPS analysis.

The peaks in the Fe 2p scan (Fig. 9e) are attributed to Fe $2p_{3/2}$ (712.4 eV, suggesting contributions from FeOOH, $Fe(OH)_3$ and other iron oxide species typically between 710.5 and 711.5 eV, and iron phosphate typically between 713 and 714 eV), Fe $2p_{1/2}$ (726.3 eV), and a satellite peak (716.4 eV) [58–60]. In Fig. 9f, the peak at 134.4 eV is assigned to phosphorus [61] while the peak at 137.0 eV likely corresponds to Pb, PbO, and $Pb(OH)_2$ [62]. While these peak positions suggest oxygen-containing metal species, the chemical complexity of the water matrix and overlapping XPS binding energies indicate that multiple metal-containing phases (phosphate, carbonates, etc.) likely coexist. The prevalence of phosphorus within the sludge might suggest that modified fibers facilitate the removal of this highly regulated contaminant, although trace amounts of this contaminant were also found in the cardboard starting material (Fig. S14). Overall, these results further suggest that metal hydroxide precipitation enables metals to become incorporated into flocs during coagulation-flocculation. Conversely, Ni and Mn (removal ~10%) were not observed on the sludge surface (Fig. S12b-c), confirming these metals did not incorporate within the flocs during treatment.

4. Conclusion and implications

In this study, quaternary ammonium modified cellulose fibers have been demonstrated as a proof-of-concept material for improving conventional coagulation–flocculation processes. The optimal oxidation time for preparing modified fibers, and the ideal fiber concentration were determined to be 60 min and 150 mg/L, respectively. The flocs formed with the modified fibers are 30 times larger and settle 4 times faster than those formed by the conventional method. Furthermore, the modified fiber-based treatment strategy outperformed the pristine fibers and conventional strategy under challenging influent conditions with both settling and screening floc separation methods. At pH 8.9, the modified fibers (150 mg/L) achieved a settled turbidity of 3.7 NTU, while pristine fibers (150 mg/L) and the conventional method only

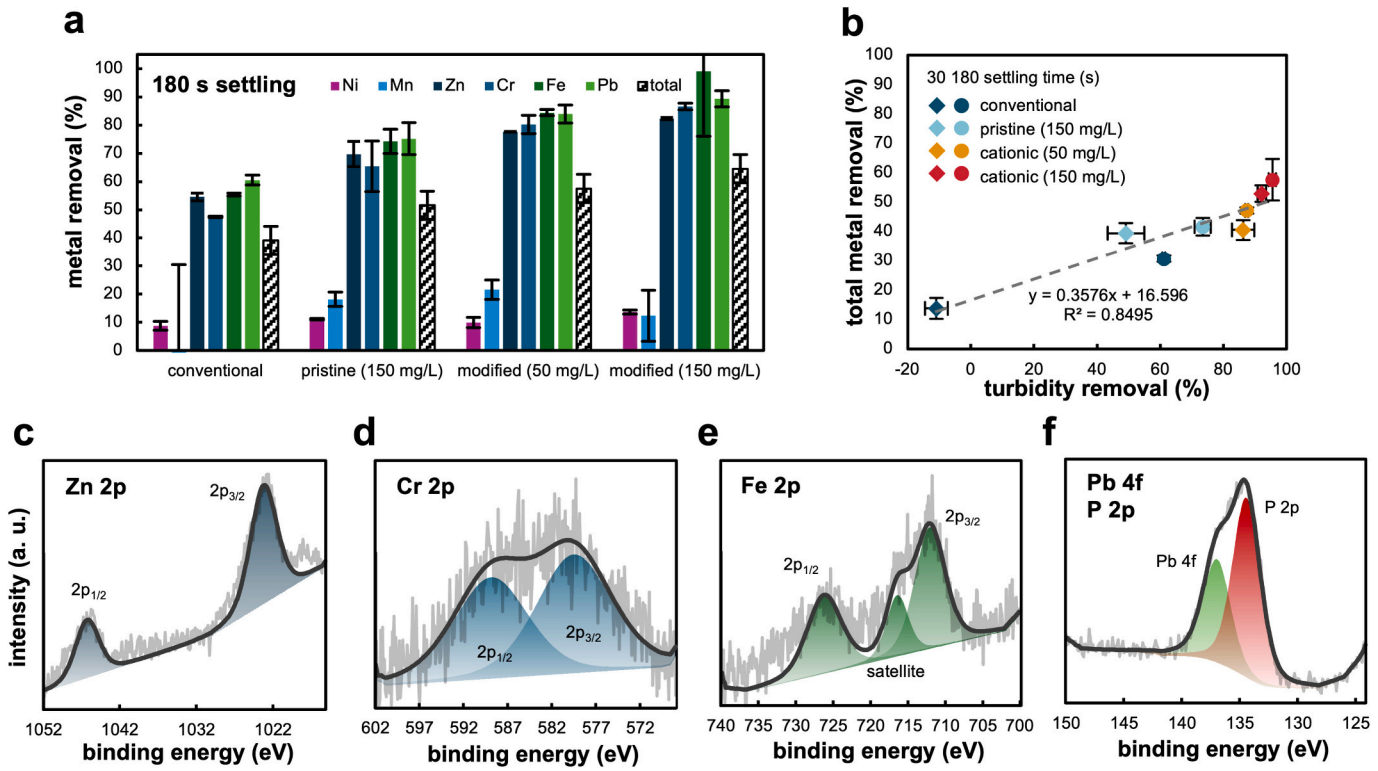

Fig. 9. (a) Removal of metals after 180 s of settling with conventional, pristine fiber-enhanced (150 mg/L), and modified fiber-enhanced (50 and 150 mg/L) treatment strategies. Initial concentrations: Mn, Cr, Pb = 0.05 mg/L and Ni, Zn, Fe = 0.5 mg/L. Coagulant and flocculant concentrations: 48 mg/L alum and 0.5 mg/L aPAM. Jar test conditions: pH = 7.7 ± 0.1, initial turbidity = 62 ± 1 NTU. (b) Relationship between total metal removal (%) and turbidity removal (%) for each treatment strategy at both 30 s (diamonds) and 180 s (circles) of settling. High resolution XPS scans of sludge after treatment with 150 mg/L modified fibers for (c) Zn 2p, (d) Cr 2p, (e) Fe 2p and (f) Pb 4f/P2p (each spectrum is the average of 50 scans). Data points and error bars are calculated from the average and standard deviation of three replicates.

reached 34 and 63 NTU, respectively. The modified fibers (150 mg/L) maintained the target turbidity even in the presence of up to 20 mM additional NaCl, while pristine fibers exceeded this limit at 10 mM NaCl. At just 50 mg/L, modified fibers performed similarly to 150 mg/L pristine fibers for all influent conditions and significantly outperformed pristine fibers for treating highly turbid influent water. Finally, the removal of heavy metals was compared, and due to the incorporation of metal hydroxide precipitates within flocs, modified fibers showed a distinct improvement compared to pristine fibers and the conventional treatment strategy.

While the use of a recycled cellulose source material holds promise for cost-effective scale-up of the technology due to its ability to be implemented within existing infrastructure, a techno-economic analysis is needed to evaluate the feasibility of full-scale implementation. Moreover, while the quaternary ammonium modification is an interesting proof-of-concept, further studies are needed to develop more cost effective and sustainable fiber modification strategies. Advancing cellulose cationization approaches such as via deep eutectic solvents [63,64], mechanochemical synthesis methods [65,66] or physical adsorption of charged polyelectrolytes [67] have strong potential to improve the scalability and sustainability of the proposed strategy. Additionally, the reusability of fibers, their degradation and fate within sludge, as well as their impact on dewaterability requires further investigation. The cationization of cellulose fibers is known to increase their degree of swelling in water [23], which may have implications on sludge dewaterability as well as biodegradability of the material at its end-of-life. Ongoing work aims to address the reusability of modified fibers, as well as improve their performance in diverse real wastewaters by mitigating the negative impacts of elevated ionic strength and dissolved organic matter through optimized fiber dosing strategies, alternative surface modifications, and/or facile pre-treatment approaches.

Declaration of competing interest

The authors declare the following financial interests/personal relationships which may be considered as potential competing interests: Nathalie Tufenkji reports financial support was provided by Canada Research Chairs Program. Nathalie Tufenkji, Owen Armstrong and Georgina Kalogerakis report financial support was provided by Natural Sciences and Engineering Research Council of Canada. Nathalie Tufenkji reports financial support was provided by Fondation canadienne pour l'innovation. Nathalie Tufenkji and Owen Armstrong report financial support was provided by McGill University. Masashi Kaneda reports financial support from the Japan Society for the Promotion of Science, the Fonds de recherche du Québec – Nature et technologies, the Rotary Foundation, and the Funai Foundation for Information Technology. Nathalie Tufenkji and Mathieu Lapointe have patent pending on the use of fiber-based materials for water treatment. If there are other authors, they declare that they have no known competing financial interests or personal relationships that could have appeared to influence the work reported in this paper.

Acknowledgment

The authors acknowledge the Canada Research Chairs Program [CRC-2022-00274], the Natural Sciences and Engineering Research Council of Canada (NSERC) CREATE MIXCHEM program [CREATE 596176-2025], the Canada Foundation for Innovation [36368, 40070, 43152], and the McGill Innovation Fund. O.A. was funded by an NSERC CGS-M scholarship and received additional support from the Brace Water Center (McGill University). M.K. thanks support from the Japan Society for the Promotion of Science, the Fonds de recherche du Québec-Nature et technologies, the Rotary Foundation, and the Funai

Foundation for Information Technology. G. K. acknowledges NSERC for a postdoctoral fellowship. The authors thank A. Golsztajn and R. Roy for technical assistance with ICP-OES and M. Verhille and A. Aoun for assistance with jar tests using real wastewater. The authors thank M. Hadioui and Professor T. van de Ven for helpful discussions during preparation of the manuscript. The authors acknowledge the support from the Sainte-Catherine Wastewater Treatment Plant (Québec, Canada) for providing municipal wastewater samples.

Appendix A. Supplementary data

Supplementary data to this article can be found online at https://doi.org/10.1016/j.seppur.2026.138125.

Data availability

The data that support the findings of this study will be deposited into a publicly available repository upon publication. A link to the repository will also be included in the final publication.

References

[1] U. N. D. of E. and S. Affairs, The sustainable development goals report 2024, United Nations (2024), https://doi.org/10.18356/9789213589755.
[2] A.A. Adegoke, I.D. Amoah, T.A. Stenström, M.E. Verbyla, J.R. Mihelcic, Epidemiological evidence and health risks associated with agricultural reuse of partially treated and untreated wastewater: a review, Front. Public Health 6 (2018), https://doi.org/10.3389/fpubh.2018.00337.
[3] M. Preisner, E. Neverova-Dziopak, Z. Kowalewski, Analysis of eutrophication potential of municipal wastewater, Water Sci. Technol. 81 (9) (2020) 1994–2003, https://doi.org/10.2166/wst.2020.254.
[4] R.P. Ribeiro, L.F.P. Alves, C.B. de Cerqueira, L.M. Mombrini, H.B.P. Ferreira, Effects of untreated or insufficiently treated wastewater discharges on the spatial and temporal variability of nitrous oxide (N2O) emissions from different streams in southeastern Brazil, Water Sci. Technol. 83 (5) (2021) 1141–1151, https://doi.org/10.2166/wst.2021.043.
[5] UNESCO, The United Nations world water development report, Wastewater: the untapped resource - UNESCO Digital Library, Accessed: Oct. 06, 2024. [Online]. Available: https://unesdoc.unesco.org/ark:/48223/pf0000247153, 2017.
[6] A.M. Michalak, et al., The frontiers of water and sanitation, Nat Water 1 (1) (2023) 10–18, https://doi.org/10.1038/s44221-022-00020-1.
[7] M. Lapointe, H. Jahandideh, J.M. Farner, N. Tufenkji, Super-bridging fibrous materials for water treatment, npj Clean Water 5 (1) (2022) 1–10, https://doi.org/10.1038/s41545-022-00155-4.
[8] M. Sillanpää, M.C. Ncibi, A. Matilainen, M. Vepsäläinen, Removal of natural organic matter in drinking water treatment by coagulation: a comprehensive review, Chemosphere 190 (2018) 54–71, https://doi.org/10.1016/j.chemosphere.2017.09.113.
[9] J. Gregory, S. Barany, Adsorption and flocculation by polymers and polymer mixtures, Adv. Colloid Interface Sci. 169 (1) (2011) 1–12, https://doi.org/10.1016/j.cis.2011.06.004.
[10] N. Wilkinson, A. Metaxas, E. Brichetto, S. Wickramaratne, T.M. Reineke, C. S. Dutcher, Ionic strength dependence of aggregate size and morphology on polymer-clay flocculation, Colloids Surf. A Physicochem. Eng. Asp. 529 (2017) 1037–1046, https://doi.org/10.1016/j.colsurfa.2017.06.085.
[11] B. Cao, B. Gao, X. Liu, M. Wang, Z. Yang, Q. Yue, The impact of pH on floc structure characteristic of polyferric chloride in a low DOC and high alkalinity surface water treatment, Water Res. 45 (18) (2011) 6181–6188, https://doi.org/10.1016/j.watres.2011.09.019.
[12] B. Azimi, et al., Application of cellulose-based materials as water purification filters; a state-of-the-art review, J. Polym. Environ. 32 (1) (2024) 345–366, https://doi.org/10.1007/s10924-023-02989-6.
[13] Y. Zhang, H. Sun, Y. Cao, M.J. Kalinowski, M. Li, B. Marelli, Directed Assembly of Proteinaceous–Polysaccharide Nanofibrils to Fabricate Membranes for Emerging Contaminant Remediation, ACS Nano 18 (36) (2024) 25205–25215, https://doi.org/10.1021/acsnano.4c07409.
[14] X. Zhang, J. Ding, Z. Li, J. Dai, N. Li, H. Li, Rapid remediation of nanoplastics from water using a novel superparamagnetic absorbent, Sep. Purif. Technol. 351 (2024) 128069, https://doi.org/10.1016/j.seppur.2024.128069.
[15] T.W. Kurniawan, H. Sulistyarti, B. Rumhayati, A. Sabarudin, Cellulose nanocrystals (CNCs) and cellulose nanofibers (CNFs) as adsorbents of heavy metal ions, J. Chem. 2023 (1) (2023) 5037027, https://doi.org/10.1155/2023/5037027.
[16] M. Lapointe, R.S. Kurusu, L.M. Hernandez, N. Tufenkji, Removal of classical and emerging contaminants in water treatment using super-bridging Fiber-based materials, ACS EST Water 3 (2) (2023) 377–386, https://doi.org/10.1021/acsestwater.2c00443.
[17] N. Haleem, et al., Preparation of cationic cellulose as a natural flocculant/sorbent and its application in three water treatment scenarios, Water 15 (11) (2023), https://doi.org/10.3390/w15112021.
[18] D. Vandamme, I. Foubert, B. Meesschaert, K. Muylaert, Flocculation of microalgae using cationic starch, J. Appl. Phycol. 22 (4) (2010) 525–530, https://doi.org/10.1007/s10811-009-9488-8.
[19] B.A. Lasaki, P. Maurer, H. Schönberger, E.P. Alvarez, Empowering municipal wastewater treatment: enhancing particulate organic carbon removal via chemical advanced primary treatment, Environ. Technol. Innovation 32 (2023) 103436, https://doi.org/10.1016/j.eti.2023.103436.
[20] H. Liimatainen, T. Suopajärvi, J. Sirviö, O. Hormi, J. Niinimäki, Fabrication of cationic cellulosic nanofibrils through aqueous quaternization pretreatment and their use in colloid aggregation, Carbohydr. Polym. 103 (2014) 187–192, https://doi.org/10.1016/j.carbpol.2013.12.042.
[21] S. Garcia-Segura, M.M.S.G. Eiband, J.V. de Melo, C.A. Martínez-Huitle, Electrocoagulation and advanced electrocoagulation processes: a general review about the fundamentals, emerging applications and its association with other technologies, J. Electroanal. Chem. 801 (2017) 267–299, https://doi.org/10.1016/j.jelechem.2017.07.047.
[22] R.S. Kurusu, M. Lapointe, N. Tufenkji, Sustainable iron-grafted cellulose fibers enable coagulant recycling and improve contaminant removal in water treatment, Chem. Eng. J. 430 (2022) 132927, https://doi.org/10.1016/j.cej.2021.132927.
[23] H. Yang, T.G.M. van de Ven, Preparation of hairy cationic nanocrystalline cellulose, Cellulose 23 (3) (2016) 1791–1801, https://doi.org/10.1007/s10570-016-0902-5.
[24] D.L.V. Brussel-Verraest, A.C. Besemer, H.J. Thiewes, A.-M.Y.W. Verwilligen, "Cationic cellulosic fibres," WO2003006739A1, Accessed: May 09, 2025. [Online]. Available: https://patents.google.com/patent/WO2003006739A1/en?oq=WO03006739, 2003.
[25] I. Petrinić, H. Bukšek, T. Luxbacher, T. Pušić, S. Bischof, Influence of the structure of polymer fiber composites on the analysis of the zeta potential, J. Appl. Polym. Sci. 135 (21) (2018) 46227, https://doi.org/10.1002/app.46227.
[26] OECD, *Test No. 303: Simulation Test - Aerobic Sewage Treatment – A: Activated Sludge Units; B: Biofilms*. in OECD Guidelines for the Testing of Chemicals, Section 3. OECD, 2001, https://doi.org/10.1787/9789264070424-en.
[27] M. Lapointe, B. Barbeau, Substituting polyacrylamide with an activated starch polymer during ballasted flocculation, J. Water Process Eng. 28 (2019) 129–134, https://doi.org/10.1016/j.jwpe.2019.01.011.
[28] MELCC, Règlement sur les ouvrages municipaux d'assainissement des eaux usées-Loi sur la qualité de l'environnement, Chapitre Q-2, r 34 (2013).
[29] O.S. Alimi, et al., Effects of weathering on the properties and fate of secondary microplastics from a polystyrene single-use cup, J. Hazard. Mater. 459 (2023) 131855, https://doi.org/10.1016/j.jhazmat.2023.131855.
[30] "2540 SOLIDS" in Standard Methods For the Examination of Water and Wastewater, 0 vols., in Standard Methods for the Examination of Water and Wastewater. American Public Health Association, 2017, https://doi.org/10.2105/SMWW.2882.030.
[31] P. Du, et al., Occurrence and fate of heavy metals in municipal wastewater in Heilongjiang province, China: a monthly reconnaissance from 2015 to 2017, Water 12, no. 3, Art. no. 3 (2020), https://doi.org/10.3390/w12030728.
[32] Q.G. Fan, D.M. Lewis, K.N. Tapley, Characterization of cellulose aldehyde using fourier transform infrared spectroscopy, J. Appl. Polym. Sci. 82 (5) (2001) 1195–1202, https://doi.org/10.1002/app.1953.
[33] Y. Wang, B.-Y. Gao, X.-M. Xu, W.-Y. Xu, G.-Y. Xu, Characterization of floc size, strength and structure in various aluminum coagulants treatment, J. Colloid Interface Sci. 332 (2) (2009) 354–359, https://doi.org/10.1016/j.jcis.2009.01.002.
[34] K. Saxena, U. Brighu, Comparison of floc properties of coagulation systems: effect of particle concentration, scale and mode of flocculation, J. Environ. Chem. Eng. 8 (5) (2020) 104311, https://doi.org/10.1016/j.jece.2020.104311.
[35] M. Qasim, S. Park, Y. Moon, J.-O. Kim, Developing a model to determine the settling velocity of ballasted flocs, J. Environ. Chem. Eng. 8 (6) (2020) 104515, https://doi.org/10.1016/j.jece.2020.104515.
[36] M. Hubert, T. Meyn, M.C. Hansen, S.E. Hale, H.P.H. Arp, Per- and polyfluoroalkyl substance (PFAS) removal from soil washing water by coagulation and flocculation, Water Res. 249 (2024) 120888, https://doi.org/10.1016/j.watres.2023.120888.
[37] M. Peydayesh, et al., Sustainable Removal of Microplastics and Natural Organic Matter from Water by Coagulation–Flocculation with Protein Amyloid Fibrils, Environ. Sci. Technol. 55 (13) (2021) 8848–8858, https://doi.org/10.1021/acs.est.1c01918.
[38] P. Wang, et al., Removal of perfluorooctanoic acid (PFOA) and perfluorooctanesulfonic acid (PFOS) by coagulation: influence of coagulant and dosing conditions, Sep. Purif. Technol. 355 (2025) 129562, https://doi.org/10.1016/j.seppur.2024.129562.
[39] E. O'Flaherty, N.F. Gray, A comparative analysis of the characteristics of a range of real and synthetic wastewaters, Environ. Sci. Pollut. Res. 20 (12) (2013) 8813–8830, https://doi.org/10.1007/s11356-013-1863-y.
[40] M.E. Bote, W.M. Desta, Removal of turbidity from domestic wastewater using electrocoagulation: optimization with response surface methodology, Chem. Afr. 5 (1) (2022) 123–134, https://doi.org/10.1007/s42250-021-00303-2.
[41] J. Gregory, Particles in water: properties and processes, Boca Raton: CRC Press (2005), https://doi.org/10.1201/9780203508459.
[42] A. Zita, M. Hermansson, Effects of ionic strength on bacterial adhesion and stability of flocs in a wastewater activated sludge system, Appl. Environ. Microbiol. 60 (9) (1994) 3041–3048, https://doi.org/10.1128/aem.60.9.3041-3048.1994.
[43] M. Hernández-Rivas, et al., Deposition of synthetic and bio-based polycations onto negatively charged solid surfaces: effect of the polymer cationicity, ionic strength,

and the addition of an anionic surfactant, Colloids and Interfaces 4, no. 3, Art. no. 3 (2020), https://doi.org/10.3390/colloids4030033.
[44] H. Wang, J. Qi, A.A. Keller, M. Zhu, F. Li, Effects of pH, ionic strength and humic acid on the removal of TiO2 nanoparticles from aqueous phase by coagulation, Colloids Surf. A Physicochem. Eng. Asp. 450 (2014) 161–165, https://doi.org/10.1016/j.colsurfa.2014.03.029.
[45] R. Wattana, D. Park, C.O. Osuji, Ion specific effects on the rheology of cellulose nanofibrils in the presence of salts, Soft Matter (2025), https://doi.org/10.1039/D5SM00339C.
[46] M. Kaneda, et al., Inhibition of silica scaling with functional polymers: role of ionic strength, divalent ions, and temperature, Water Res. 258 (2024) 121705, https://doi.org/10.1016/j.watres.2024.121705.
[47] E. Jafari, M.R. Malayeri, H. Brückner, P. Krebs, Impact of operating parameters of electrocoagulation-flotation on the removal of turbidity from synthetic wastewater using aluminium electrodes, Miner. Eng. 193 (2023) 108007, https://doi.org/10.1016/j.mineng.2023.108007.
[48] M. Lapointe, C.M. Rochman, N. Tufenkji, Sustainable strategies to treat urban runoff needed, Nat Sustain 5 (5) (2022) 366–369, https://doi.org/10.1038/s41893-022-00853-4.
[49] F. Blancho, M. Lapointe, A.C. Quevedo, K. Kannan, N. Tufenkji, Demonstrating scale-up of a novel water treatment process using super-bridging agents, Water Res. 254 (2024) 121301, https://doi.org/10.1016/j.watres.2024.121301.
[50] J.-C. Lee, Y.-O. Son, P. Pratheeshkumar, X. Shi, Oxidative stress and metal carcinogenesis, Free Radic. Biol. Med. 53 (4) (2012) 742–757, https://doi.org/10.1016/j.freeradbiomed.2012.06.002.
[51] J.F. Blais, Z. Djedidi, R.B. Cheikh, R.D. Tyagi, G. Mercier, Metals precipitation from effluents: review, Practice Periodical of Hazardous, Toxic, and Radioactive Waste Management 12 (3) (2008) 135–149, https://doi.org/10.1061/(ASCE)1090-025X(2008)12:3(135).
[52] V. Choudhary, D.W. Boukhvalov, L. Philip, Role of inner-sphere complexation in phosphate removal by metal–organic frameworks: experimental and theoretical investigation, Environ. Sci.: Water Res. Technol. 9 (2) (2023) 572–585, https://doi.org/10.1039/D2EW00636G.
[53] Y. Song, H.H. Hahn, E. Hoffmann, Effects of solution conditions on the precipitation of phosphate for recovery: a thermodynamic evaluation, Chemosphere 48 (10) (2002) 1029–1034, https://doi.org/10.1016/S0045-6535(02)00183-2.
[54] M. Wang, L. Jiang, E. Jung Kim, S. Hong Hahn, Electronic structure and optical properties of Zn(OH) 2 : LDA+ U calculations and intense yellow luminescence, *RSC* Adv. 5 (106) (2015) 87496–87503, https://doi.org/10.1039/C5RA17024A.
[55] M.C. Biesinger, B.P. Payne, A.P. Grosvenor, L.W.M. Lau, A.R. Gerson, R. St, C. Smart, Resolving surface chemical states in XPS analysis of first row transition metals, oxides and hydroxides: Cr, mn, fe, co and ni, Appl. Surf. Sci. 257 (7) (2011) 2717–2730, https://doi.org/10.1016/j.apsusc.2010.10.051.
[56] B.A. Manning, J.R. Kiser, H. Kwon, S.R. Kanel, Spectroscopic investigation of Cr (III)- and Cr(VI)-treated nanoscale zerovalent iron, Environ. Sci. Technol. 41 (2) (2007) 586–592, https://doi.org/10.1021/es061721m.
[57] W. Liu, et al., Different pathways for Cr(III) oxidation: implications for Cr(VI) reoccurrence in reduced chromite ore processing residue, Environ. Sci. Technol. 54 (19) (2020) 11971–11979, https://doi.org/10.1021/acs.est.0c01855.
[58] R. Natarajan, N. Palaniswamy, M. Natesan, V.S. Muralidharan, XPS analysis of passive film on stainless steel, TOCORRJ 2 (1) (2009) 114–124, https://doi.org/10.2174/1876503300902010114.
[59] M.A. Salim, G.D. Khattak, P.S. Fodor, L.E. Wenger, X-ray photoelectron spectroscopy (XPS) and magnetization studies of iron–vanadium phosphate glasses, J. Non Cryst. Solids 289 (1) (2001) 185–195, https://doi.org/10.1016/S0022-3093(01)00727-X.
[60] Y. Wang, P.M.A. Sherwood, Iron (III) phosphate (FePO4) by XPS, Surf. Sci. Spectra 9 (1) (2003) 99–105, https://doi.org/10.1116/11.20030106.
[61] X. Wu, K. Gong, G. Zhao, W. Lou, X. Wang, W. Liu, Mechanical synthesis of chemically bonded phosphorus–graphene hybrid as high-temperature lubricating oil additive, RSC Adv. 8 (9) (2018) 4595–4603, https://doi.org/10.1039/C7RA11691H.
[62] Z. Liu, J. Shi, D. Ji, X. Zhang, B. Sun, Deposition behavior of lead in lead methanesulfonate flow batteries with the addition of tin(II) methanesulfonate, J. Electrochem. Soc. 168 (7) (2021) 070545, https://doi.org/10.1149/1945-7111/ac132c.
[63] X.-Y. Ye, E.-Q. Zhu, D.-W. Wang, J. Yang, H.-Y. Yang, Z.-J. Shi, Cationic functionalized bamboo fibers with spinnable and antibacterial properties prepared in chlorocholine chloride/urea deep eutectic solvent, Ind. Crop. Prod. 188 (2022) 115607, https://doi.org/10.1016/j.indcrop.2022.115607.
[64] Z. Yang, T.-A. Asoh, H. Uyama, Cationic functionalization of cellulose monoliths using a urea-choline based deep eutectic solvent and their applications, Polym. Degrad. Stab. 160 (2019) 126–135, https://doi.org/10.1016/j.polymdegradstab.2018.12.015.
[65] T. Nikonovich, et al., Solid-state synthesis of cationic cellulose fibers from low-processed cotton for efficient virus capture, ACS Sustain. Chem. Eng. (2025), https://doi.org/10.1021/acssuschemeng.5c07884.
[66] G. Yang, et al., Low-energy synthesis of individualized pH-responsive cationic cellulose nanofibers and chitin nanocrystals by mechanochemistry and aging, Nanoscale Horiz. (2025), https://doi.org/10.1039/D5NH00597C.
[67] C. Sampl, J. Schaubeder, U. Hirn, S. Spirk, Interplay of electrolyte concentration and molecular weight of polyDADMAC on cellulose surface adsorption, Int. J. Biol. Macromol. 239 (2023) 124286, https://doi.org/10.1016/j.ijbiomac.2023.124286.